J Therm Anal Calorim (2013) 112:689–695
DOI 10.1007/s10973-012-2613-y

Glass transition, fragility, and structural features of amorphous nickel–tellurate–vanadate samples

Dariush Souri · Seyed Ali Salehizadeh

Received: 4 August 2011 / Accepted: 16 July 2012 / Published online: 26 August 2012
© Akadémiai Kiadó, Budapest, Hungary 2012

Abstract The experimental FTIR spectra and DSC curves of the ternary $40TeO_2$–$(60-x)V_2O_5$–xNiO glasses with $0 \leq x \leq 30$ (in mol%) have been investigated. The glass transition properties that have been measured and reported in this paper, include the glass transition temperature (T_g), glass transition width (ΔT_g), heat capacity change at glass transition (ΔC_P) and Fragility (F). Thermal stability, fragility, and glass-forming tendency of these glasses have been estimated. Also, Poisson's ratio (μ) and IR spectra of the presented systems have been investigated, to determine relationship between chemical composition and the thermal stability or to interpret the structure of glass. In addition, Makishima and Makenzie's theory was applied for determination of Young's modulus, bulk modulus, and shear modulus, indicating a strong relation between elastic properties and structure of glass. In general, results of this work show that glasses with $x = 0$ and 30 have the highest shear and young's modulus which make them as suitable candidate for the manufacture of strong glass fibers in technological applications; but it should be mentioned that glass with $x = 30$ has higher handling temperature and super resistance against thermal shock.

Keywords Differential scanning calorimetry · Fourier transform infrared spectroscopy · Glass transition · Young's modulus · Fragility

D. Souri (✉)
Faculty of Science, Department of Physics, Malayer University, Malayer, Iran
e-mail: d.souri@gmail.com; d.souri@malayeru.ac.ir

S. A. Salehizadeh
Department of Physics, Varamin-Pishva Branch, Islamic Azad University, Varamin, Iran

Introduction

TeO_2-based glasses have a technical and scientific interest because of their low melting temperature, no hygroscopic property, good infrared transmission, electrical properties, optical properties and thermopower features [1–13]. Study in structural characteristics of glasses by spectral analyzing, DSC curve and elastic modulus can be a suitable way to understand the behavior of glasses as a function composition [14]. The role of changing in glass composition on the polarization power of network formers, modifiers, their coordination numbers, the concentration of non-bridging oxygen, rigidity, and packing of glass can help us to reach to optimized combination satisfying high thermal stability against thermal shocks for technological applications.

Nickel oxide (NiO) is an interesting material due to its useful electronic, magnetic, and catalytic properties [15]. NiO has also become very important for it can be used as electrode material in battery systems [16]. To the best of our knowledge, there are some papers on the calorimetric, structural, and physical properties of TeO_2-based glasses and then, tricomponent glass systems of the form A_mO_n–TeO_2–V_2O_5 (A_mO_n is an another oxide) have been studied [3, 4, 17–19]; in this work, due to the importance of the binary TeO_2–V_2O_5 glass, the structural and calorimetric properties of V_2O_5–NiO–TeO_2 glasses are studied, searching for glasses having high thermal stability; thus, in this work, we are going to follow two aims, first is the study of FTIR spectra and DSC curves of the ternary tellurite-vanadate glasses containing nickel oxide, to introduce samples with higher thermal stability, and second is finding logical correlation between thermal and structural characters and also application of Makishima and Mackenzie's theory.

Experimental procedure

The ternary $40TeO_2$–$(60-x)V_2O_5$–xNiO glass systems with $0 \leq x \leq 30$ (in mol%), hereafter, termed as TVNx, were prepared by rapid melt quenching method. The details of these sample preparation and their XRD patterns can be found in our previous work [4]. Also, the glass transition temperature (T_g) of these samples were obtained using differential scanning calorimetry (DSC: Pyris1, USA) which increase with increasing of NiO content and was in the range 249.3–356.3 °C. The FTIR absorption spectra of the produced glass samples were recorded at room temperature on a Perkin Elmer Spectrum RX/I FT-IR System(USA) over a spectral range of 400–4,000 cm^{-1}. First, disks of KBr, 1 cm in diameter, were prepared by pressing, and their infrared absorption spectra measured, showed transparency to light. Then, potassium bromide (KBr)-glass pressed powder pellets were used at 1:30 volume ratio of glass to KBr (preparation of pellets with high IR transmission) to collect the IR spectra and using these results, we are able to determine structural units.

Results and discussion

Differential scanning calorimetry (DSC)

Figure 1 shows the DSC charts obtained for the TVNx glasses; for better clarity of the plots, DSC charts have been plotted separately.

The DSC curves for the glasses show a glass transition correspond to temperature T_g that we usually just take the middle of the incline to be the T_g. This transition is followed by one exothermic peak corresponding to crystallization temperature T_{cr}; in other word, DSC measurements show a pronounced crystallization exotherm after the glass transition temperature indicating the glassy nature of the materials at temperature below the glass transition. No indication of T_{cr} was observed in DSC spectrum of TVN30 in the studied temperature range (0–600 °C). The data of T_g, T_{cr}, glass transition width ($\Delta T_g = T_{g.end} - T_{g.onset}$, where $T_{g.end}$ and $T_{g.onset}$ are the end point and start point of endothermic part of DSC curve corresponding to glass transition phenomenon) and heat capacity change at glass transition (ΔC_P) are presented in Table 1; ΔC_P values of these glasses have been reported only at transition temperature during the DSC experiment. Figure 2 shows the variation of the glass transition temperature with NiO content in the TVNx samples. From this figure, one sees that the glass transition temperature is very sensitive to the NiO concentration. The addition of NiO to vitreous TeO_2–V_2O_5 from 0 to 30 mol% results in a regular increase of T_g from 249.32 to 365.30 °C. Such a result was reported also for vanadium telluride blown film glasses [20]. Increasing of T_g can be interpreted as increasing of the rigidity of the glass; in other word, the change in T_g for different samples is related to the structure of each glass, arising from the interaction between the three oxides; this statement has been justified upon the FTIR results, presented in "Fourier transform infra-red analysis". Thermal stability depends on $\Delta T = T_{Cr} - T_g$, where T_{Cr} is crystallization temperature [18, 19, 21–24]. Upon the data of T_g, $T_{Cr,}$ and ΔT (i.e., Table 1), it is obvious that ΔT increase with increasing NiO content; hence, it can be predicted that the thermal stability of these glasses will be >80 and 67 K, which were the highest thermal stability measured for CoO–V_2O_5–TeO_2 [18] and V_2O_5–Fe_2O_3–TeO_2 [19], respectively; since T_g and T_{Cr} are the characteristic temperatures of any glass and T_{Cr} can not be spotted within the studied temperature range for TVN30, it can be therefore expected that the T_{Cr} value of this glass must be above 600 °C (higher ΔT between other TVNx glasses), which make it strong against thermal shocks. The variation of the excess heat capacity, ΔC_P, in the present system at the glass transition temperature as a function of composition is shown in Fig. 3. It can be seen in Fig. 3 that ΔC_P decreases with increasing NiO concentration. In general, a smaller ΔC_P is a characteristic feature of a fragile glass which has larger glass-forming tendency and a higher ΔC_P corresponds to a strong glass which has a smallest glass-forming tendency [25–28]. The thermodynamic fragility, F, can be calculated by using the relation:

$$F = \frac{0.151 - \chi}{0.151 + \chi} \quad (1)$$

where $\chi = \Delta T_g / T_g$ [25, 29]; ΔT_g data have been listed in Table 1. The variation of thermodynamic fragility with NiO content is shown in Fig. 3 for these glasses. Thermodynamic fragility is found to increase with increasing NiO content. This can be attributed to the glass network getting loosely packed with increasing of NiO content.

A similar conclusion has been drawn in the case of CoO–V_2O_5–TeO_2 [18]. However, the glass-forming tendency increases with increasing NiO content.

Fourier transform infrared analysis (FTIR)

The structure of the glasses was also studied using FTIR analysis in the wave number range 400–4,000 cm^{-1}. There are no characteristic absorption bands in the range 1,150–4,000 cm^{-1}, only shallow oscillations due to interference effects in the glass; bands at 2,356 and 2,900 cm^{-1} are associated to the aparatus's background absorption. Figure 4 shows FTIR spectra of TVNx glasses in the range 400–1,200 cm^{-1}. For comparison, the absorption bands of KBr pellets of individual pure powders are also presented in Table 2. Comparison of the absorption bands of all the

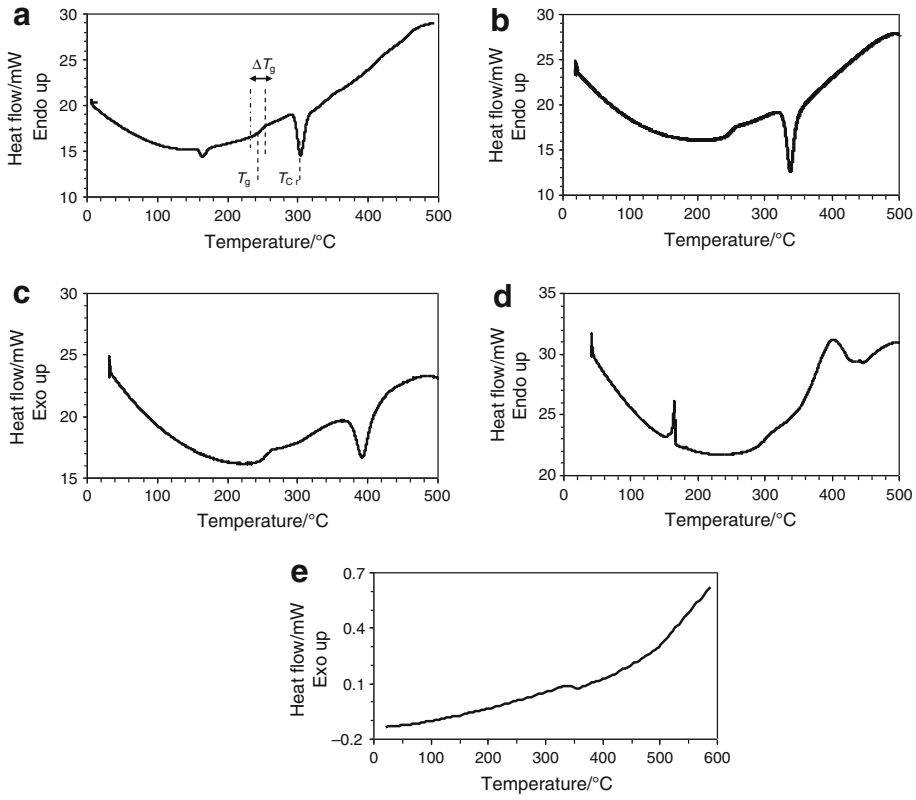

Fig. 1 DSC curves of **a** TVN0, **b** TVN5, **c** TVN10, **d** TVN20, and **e** TVN30 (for better clarity are shown separately)

Table 1 Values of density ρ, excess heat capacity at transition temperature ΔC_P, glass transition temperature T_g, crystallization temperature T_{Cr}, Fragilty F, molar volume V_m, Poisson's ratio μ_{cal}, Young's modulus E, bulk modulus K, shear modulus S, and other needed parameters for TVNx glasses

Glass	ρ/g cm $^{-3}$ [4]	ΔC_P/Jg^{-1} °C^{-1}	T_g/°C	T_C/°C	$T_g - T_{Cr}$/°C	ΔT_g/°C	F	V_m/cm^3 mol^{-1} [4]	μ_{cal}	E/GPa	K/Gpa	S/GPa
TVN0	3.856	0.486	249.32	304.35	55.03	18	0.353	44.858	0.270	76.593	55.607	30.144
TVN5	3.872	0.369	254.55	339.51	84.96	15	0.439	43.289	0.267	76.085	54.325	30.036
TVN10	3.900	0.297	258.08	392.90	134.82	12	0.529	41.604	0.263	75.550	53.036	29.919
TVN20	4.019	0.263	297.84	452.31	154.46	10	0.636	37.703	0.258	75.460	51.886	30.001
TVN30	4.243	0.192	365.30	–	–	9	0.719	33.189	0.255	76.113	51.787	30.322

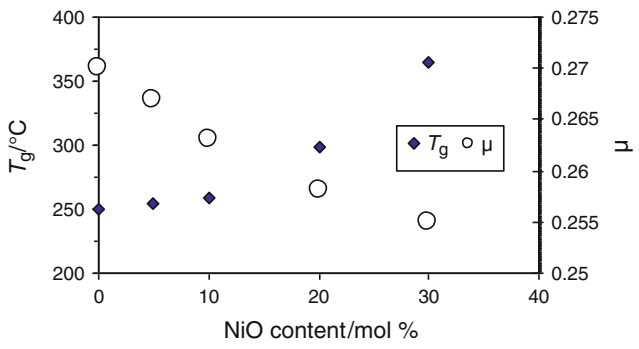

Fig. 2 Variations of glass transition temperature and Poisson's ratio for TVNx glasses

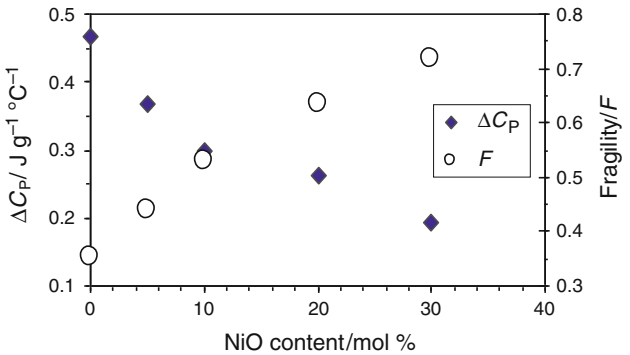

Fig. 3 Variations of excess heat capacity and fragility of TVNx glasses

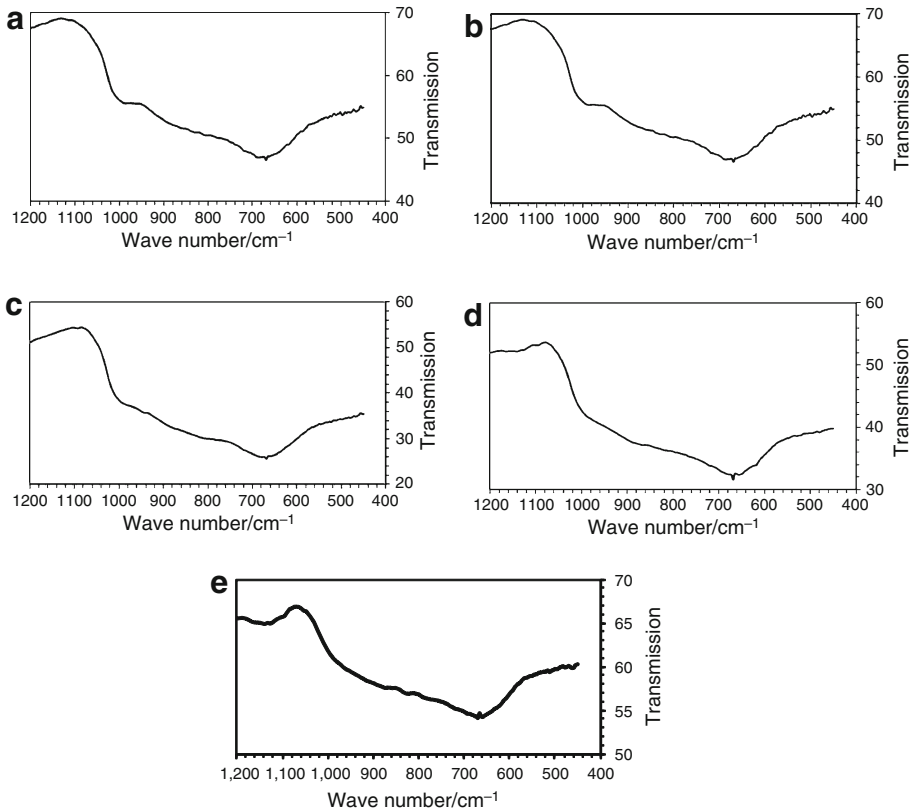

Fig. 4 FTIR spectra of **a** TVN0, **b** TVN5, **c** TVN10, **d** TVN20, and **e** TVN30 (for better clarity are shown separately); see Table 2

ternary glass systems and individual oxide powders reveal that, the FTIR spectra of the glass systems are not characteristics of a mixture of the three oxides. We suggest that, this property of the spectra indicates a chemical interaction between the three oxides [29–32]. The similarity between the FTIR spectra of all glasses indicates a similarity in their networks. In compare with the results obtained previously [14, 20, 32, 33], we suggest that the glass structure is continuous tellurite network with vanadate and nickel discontinuous. The absorption band in pure tellurium oxide powder is at 677 cm^{-1}. During the addition of other oxides and making glasses, this band changes to a shoulder (655–682 cm^{-1}). Also pure tellurite glasses have an IR absorption band at 640 cm^{-1} which is attributed to TeO_4 tetragonal pyramids [20, 22, 34]. The major observed absorption bands in the ternary TeO_2–V_2O_5–NiO glass system are summarized in Table 2. It is clear from Fig. 4 and Table 2 that the 640 cm^{-1} which is characteristics of pure TeO_2 glass, changes to a broad band and shifts from 640 to 665–678 cm^{-1} on addition of V_2O_5 and NiO. Dimitriev et al. [20] attributed this absorption band, 665–680 cm^{-1}, to TeO_3 trigonal pyramids. The weakness of this band may be due to decrease of the amount of 4-coordinate tellurium in the studied glasses (increasing of non-bridging oxygens). It is suggested that the 3-coordinated Te may become significant with increasing the concentration of V_2O_5. In the TeO_2 glasses containing

Table 2 Observed FTIR absorption bands in TVNx glasses

Glass	FTIR absorption bands/cm^{-1}
TeO_2–glass [36]	640, 774
TVN0	662, 968, 814, 1158
TVN5	474, 668, 814, 968, 1104
TVN10	470, 668, 802, 930, 1076
TVN20	472, 668, 838, 1064, 1124
TVN30	458, 502, 658, 806, 830, 1120
Pure V_2O_5 powder	588, 831, 1024
Pure TeO_2 powder	677, 775
Pure NiO powder	774, 988, 1376, 1426, 1001

60 mol% V_2O_5, a new band is observed at about 1,158 cm^{-1}, which shifts to lower wave numbers with decreasing the concentration of V_2O_5. This peak is probably attributed to V=O band of VO_5 group [14, 33, 35]. So, in contrast to Dimitriev observation, its intensity does not significant frequency and is due to the presence of V^{5+} ions; these ions have coordinated by five oxygen. The VO_5 fragments may be attached to other metal ions via V=O double bonds or V–O single bonds.

Chopra et al. [33] reported that the intensity of the band decreases with decreasing the V^{5+} ions and increasing V^{4+} ions (increasing of V^{4+}/V_{tot} fraction). Also, the peak shifts to lower wave number with decreasing the content of

V_2O_5. Such lowering in stretching frequency may be the second reason of the observation of the new band at about 1,158 cm^{-1}, which shifts to lower wave numbers.

Addition of NiO besides V_2O_5 in TeO_2 glass, cause another complex situation in the spectra. Oxygen deficiency and the presence of V^{4+} in the mixed oxides lead to the simultaneous formation of VO_6 and VO_5 polyhedra with several short V–O bonds. This is probably, the reason for a new shoulder observed at about 1,120 cm^{-1} for TVNx glasses with $x \geq 10$ mol%. The absorption band at 830–988 cm^{-1} arises due to Ni–O bonds [36]. Therefore, it is suggested that the similarity between the IR spectra of all glasses indicates a similarity in the network of these samples, namely continuous tellurite network with vanadate and nickle discontinuous.

Elastic modulus and Poisson's ratio

There is a famous model to determine elastic properties of glasses: Makashima–Mackenzie's model.

It is known that the young's modulus of crystalline oxides is given by:

$$E = \frac{2\alpha U}{r_o^3} \tag{2}$$

where α is the made lung constant, U is electrostatic energy and r_o is the interatomic distance. In the vitreous materials, as a consequence of disorder nature, we cannot define madelung constant as for crystalline oxides.

Based on Makashima–Meckenzie's model, first we introduce the packing factor of oxide $M_xO_y(V_i)$ and the packing density of glass (V_t) as:

$$V_i = \frac{4}{3}\pi N_A(x.R_M^3 + y.R_O^3) \tag{3}$$

$$V_t = V_M^{-1}\sum(x_i.V_i) \tag{4}$$

where R_M and R_O are the respective Pauling's ionic radius of metal M and oxygen O, N_A is Avogadro's number, V_M the molar volume of glass, x_i the mole fraction of oxide component i; the values of V_M have been taken from our previous paper [4]. So Young's modulus E of oxide glasses can be revealed in term of the packing density of glass V_t and the dissociation energy per unit volume G_t, as [37]:

$$E = 2\,V_t.\,G_t \tag{5}$$

In above equation, G_t is determined by:

$$G_t = \sum(x_i.G_i) \tag{6}$$

where G_i is dissociation energy per unit volume of the ith oxide.

Thus, we can obtain some of the elastic parameters such as bulk modulus K and shear modulus S as:

$$K = 1.2V_tE = 2.4V_t^2G_t \tag{7}$$

$$S = \frac{3EK}{(9K - E)} \tag{8}$$

The calculated values of Young's modulus, Shear modulus, bulk modulus and molar volume are presented in Table 1. In these evaluations, the values of dissociation energy of oxides have been taken from [38, 39], which are 54, 69.5, and 82.21 J m^{-3} for TeO_2, V_2O_5, and NiO, correspondingly. It is known that Poisson's ratio is defined by the ratio of the transverse (lateral) to the longitudinal (axial) strain, and the lateral strain would be smaller in loosly packed glasses because there is more space for atoms to move in [34]. This means that Poisson's ratio is small if atoms are loosely packed in the oxide glass whereas tightly packed glass has a higher Piosson's ratio. Theoretically, Poisson's ratio calculated from the expression given by Makishima and Makenzie [17, 37] as

$$\mu_{cal} = 0.5 - \frac{1}{7.2V_t} \tag{9}$$

Results show the decrease in Poisson's ratio from 0.270 to 0.255 as shown in Fig. 2. This result justifies the results of ΔC_P and fragility.

As seen from Table 1 and Figs. 5 and 6, bulk modulus is higher than that of SiO_2–Na_2O–B_2O_3 glasses [23]. Insertion of the modifier NiO with low content 0–10 mol% will

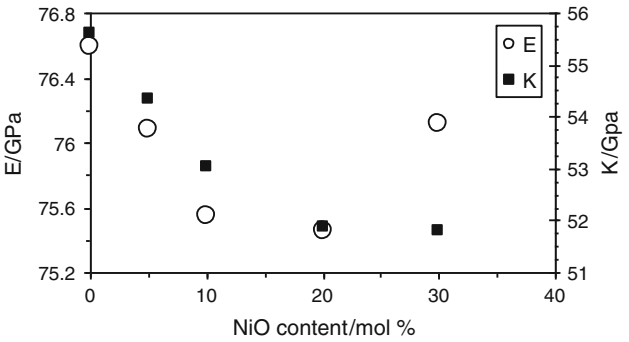

Fig. 5 Variations of Young's modulus E and bulk modulus K for TVNx glasses

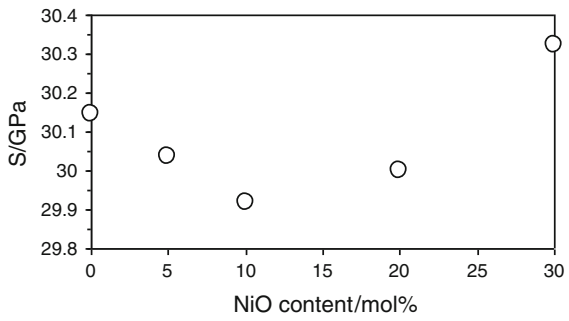

Fig. 6 Variation of shear modulus for TVNx glasses

cause a rapid decrease in elastic moduli suggesting the decrease in the average number of bonds per unit volume. The addition of NiO content up to 30 mol%, will result the increase in E and S. Figures 5 and 6 show the variation of shear and Young's moduli with NiO content. The behavior of both shear and Young's moduli show rapid decrease from 30.144 and 76.593 GPa to 29.919 and 75.550 Gpa, respectively with the increase of NiO content from 0 to 10 mol%. Upon the increase of NiO concentration to 30 mol%, both shear and Young's moduli show increasing to 76.113 and 30.322 Gpa, respectively. It is clear from the above results that the type of bonding in the network structure plays a dominant role in deciding the rigidity of these glass structures. It is believed that the behavior of both shear and Young's moduli are associated with the change in cross-linkage and coordination of the glass network [23]. Bulk modulus and Poisson's ratio decreased with the increase of NiO content.

In general, results of this work show that glasses with $x = 0$ and 30 have the highest shear and young's modulus which make them as suitable candidate for the manufacture of strong glass fibers in technological applications; but it should be mentioned that glass with $x = 30$ has probably higher handling temperature and super resistance against thermal shock, because of (a): it has the highest glass transition temperature, which makes it stronger against structural changes [18, 19, 39] and (b): glasses with higher thermal stability have higher resistance against heat shocks; on the other hand, thermal stability depends on $\Delta T = T_{Cr} - T_g$ [18, 19, 21–24]; thus, as presented in Fig. 1 and Table 1, ΔT increase with increasing of NiO content (For TVN30, T_{Cr} has not shown because it is larger than 600 °C and therefore, its ΔT is larger than that of other TVNx samples). Finally, TVN30 has the highest thermal stability, and (c): a higher value of elastic moduli is somewhat in accordance with lower thermal expansion [39], which imply to higher resistance against thermal shocks.

Conclusions

The density, elastic properties, FTIR studies, and thermal properties on the network structure of TVNX glasses reveal the following conclusions:

1. The density of the glass system studied increases with an increase in mol percentage of NiO.
2. Elastic moduli of these glasses have minima at NiO content about 10 mol%.
3. Analysis of the FTIR spectra shows an increase in the fraction of non-bridging oxygens (NBO's) with an increase of NiO content.
4. Bulk modulus and Poisson's ratio decreased with the increase of NiO content.
5. Results of this work show that glasses with $x = 0$ and 30 have the highest shear and young's modulus which make them as suitable candidate for the manufacture of strong glass fibers in technological applications; but it should be mentioned that glass with $x = 30$ has higher handling temperature and super resistance against thermal shock.

References

1. El-Mallawany R. Devitrification and vitrification of tellurite glasses. J Mater Sci. 1995;6:1–3.
2. Souri D. Small polaron hopping conduction in tellurium based glasses containing vanadium and antimony. J Non Cryst Solids. 2010;356:2181–4.
3. Souri D, Shomalian K. Band gap determination by absorption spectrum fitting method (ASF) and structural properties of different compositions of (60-x) V_2O_5–40TeO_2–xSb_2O_3 glasses. J Non Cryst Solids. 2009;355:1597–601.
4. Souri D, Salehizadeh SA. Effect of NiO content on the optical band gap, refractive index, and density of TeO_2–V_2O_5–NiO glasses. J Mater Sci. 2009;44:5800–5.
5. El-Mallawany R, Abdalla MD, Ahmed IA. New tellurite glasses: optical properties. Mater Chem Phys. 2008;109:291–6.
6. Souri D, Elahi M. The dc electrical conductivity of semiconducting TeO_2–V_2O_5–MoO_3 bulk glasses. Phys Scr. 2007;75:219–26.
7. El-Mallawany R, Saunders GA. Elastic properties of binary, ternary and quaternary rare earth tellurite glasses. J Mater Sci Lett. 1988;7:870–4.
8. Chowdari BVR, Kumari PP. Effect of mixed glass-formers in $Ag_2O{\cdot}MoO_3{\cdot}TeO_2$ system. J Phys Chem Solids. 1997;58:515–25.
9. Pal M, Hirota K, Tsujigami Y, Sakata H. Structural and electrical properties of MoO_3–TeO_2 glasses. J Phys D Appl Phys. 2001;34:459–64.
10. Sharma BK, Dube DC, Mansingh A. Preparation and characterization of V_2O_5–B_2O_3 glasses. J Non Cryst Solids. 1984;65:39–51.
11. Murugan GS, Ohishi Y. TeO_2–BaO–SrO–Nb_2O_5 glasses: a new glass system for waveguide devices applications. J Non Cryst Solids. 2004;341:86–92.
12. Jayaseelan S, Muralidharan P, Venkateswarlu M, Satyanarayana N. Transport and solid state battery characteristic studies of silver based super ion conducting glasses. Mater Sci Eng B. 2005;118:136–43.
13. Mosner P, Vosejpkova K, Koudelka L, Benes L. Thermal studies of ZnO–B_2O_3–P_2O_5–TeO_2 glasses. J Therm Anal Calorim. 2012;107(3):1129–35.
14. Turky G, Dawy M. Spectral and electrical properties of ternary (TeO_2–V_2O_5–Sm_2O_3) glasses. Mater Chem Phys. 2002;77:48–59.
15. Wi L, Wi Y, Wei H, Shi Y, Hu C. Synthesis and characteristics of NiO nanowire by a solution method. Mater Lett. 2004;58:2700–3.
16. Patil PS, Kadam LD. Preparation and characterization of spray pyrolyzed nickel oxide (NiO) thin films. Appl Surf Sci. 2002;199:211–21.
17. El-Moneim AA. DTA and IR absorption spectra of vanadium tellurite glasses. Matter Chem Phys. 2002;73:318–22.
18. Kumatso T, Noguchi T, Benino Y. Heat capacity changes and structural relaxation at glass transition in mixed-alkali tellurite glasses. J Non Cryst Solids. 1997;222:206–11.

19. El-Desoky MM, Tashtoush NM, Habib MH. Characterization and electrical properties of semiconducting Fe_2O_3–Bi_2O_3–$K_2B_4O_7$ glasses. J Mater Sci. 2005;16:533–9.
20. Dimitriev Y, Dimitrov V, Arnaudov M, Tpalov D. Ir-spectral study of vanadate vitreous system. J Non Cryst Solids. 1983;57:147–56.
21. Kumar MP, Sankarappa T, Awasthi AM. Thermal and electrical properties of some single and mixed transition-metal ion-doped tellurite glasses. Phys B. 2008;403:4088–95.
22. Zhu D, Ray CS, Zhou W, Day DE. Glass transition and fragility of Na_2O–TeO_2 glasses. J Non Cryst Solids. 2003;319:247–56.
23. Gaafar MS, Marzouk SY. Mechanical and structural studies on sodium borosilicate glasses doped with Er_2O_3 using ultrasonic velocity and FTIR spectroscopy. Phys B. 2007;388:294–302.
24. Sega K, Kuroda Y, Sakata H. DC conductivity of V_2O_5–MnO–TeO_2 glasses. J Mater Sci. 1998;33:1303–8.
25. Angell CA. Spectroscopy simulation and scattering, and the medium range order problem in glass. J Non Cryst Solids. 1985;73:1–17.
26. Sulowska J, Waclawska I, Szumera M. Effect of copper addition on glass transition of silicate–phosphate glasses. J Therm Anal Calorim 2012. doi:10.1007/s10973-012-2328-0.
27. Kumar R, Sharma P, Rangra VS. Kinetic studies of bulk $Se_{92}Te_{8-x}Sn_x$ ($x = 0, 1, 2, 3, 4$ and 5) semiconducting glasses by DSC technique. J Therm Anal Calorim. 2012;109(1):177–81.
28. Sharma A, Barman PB. Effect of Bi incorporation on the glass transition kinetics of $Se_{85}Te_{15}$ glassy alloy. J Therm Anal Calorim. 2009;96(2):413–7.
29. Ito K, Moynihan CT, Angell CA. Thermodynamic determination of fragility in liquids and a fragile-to-strong liquid transition in water. Nature. 1999;398:492–5.
30. Rao KJ, Kumar S, Bhat MH. A chemical approach to understand fragilities of glass-forming liquids. J Phys Chem B. 2001;105:9023–7.
31. Bhat H, Ganguli M, Rao KJ. Investigation of the mixed alkali effect in boro-tellurite glasses—the role of NBO–BO switching in ion transport. Curr Sci. 2004;86:676–91.
32. Pal M, Tsujigami Y, Yoshikado A, Sakata H. Electrical and optical properties of MoO_3–TeO_2 amorphous films prepared by PVD method. Phys Stat Sol (a). 2000;182:727–36.
33. Chopra N, Mansingh A, Chadha GK. Electrical, optical and structural properties of amorphous V_2O_5–TeO_2 blown films. J Non Cryst Solids. 1990;126:194–201.
34. Sinclair RN, Wrigth AC, Bachra B, Dimitriev YB, Dimitrov VV, Arnaudov MG. The structure of vitreous V_2O_5–TeO_2. J Non Cryst Solids. 1998;232–234:38–43.
35. Rajendran V, Palanivelu N, Chaudhuri BK, Goswami K. Characterisation of semiconducting V_2O_5–Bi_2O_3–TeO_2 glasses through ultrasonic measurements. J Non Cryst Solids. 2003;320:195–209.
36. Sinclair RN, Wright AC, Bachra B, Dimitriev Y, Dimitrov V, Arnaudov M. The structure of vitreous V_2O_5–TeO_2. J Non Cryst Solids. 1998;232:234–8.
37. Makishima A, Makenzie JD. Calculation of bulk modulus, shear modulus and poisson's ratio of glass. J Non Cryst Solids. 1975;12:147–57.
38. Lide DR. CRC handbook of chemistry and physics. 88th ed. Boca Raton: CRC press; 2008.
39. Inaba S, Oda S, Morigani K. Heat capacity of oxide glasses at high temperature region. J Non Cryst Solids. 2003;325:258–66.